Current Biology 19, 768–773, May 12, 2009 ©2009 Elsevier Ltd All rights reserved DOI 10.1016/j.cub.2009.03.022

Report

Bcl-2 Proteins EGL-1 and CED-9 Do Not Regulate Mitochondrial Fission or Fusion in *Caenorhabditis elegans*

David G. Breckenridge,[1,3,*] Byung-Ho Kang,[2,3] and Ding Xue[1,*]

[1]Department of Molecular, Cellular, and Developmental Biology
University of Colorado
Boulder, CO 80309
USA

[2]Department of Microbiology and Cell Science
Interdisciplinary Center for Biotechnology Research
University of Florida
Gainesville, FL 32611
USA

Summary

The Bcl-2 family proteins are critical apoptosis regulators that associate with mitochondria and control the activation of caspases. Recently, both mammalian and *C. elegans* Bcl-2 proteins have been implicated in controlling mitochondrial fusion and fission processes in both living and apoptotic cells. To better understand the potential roles of Bcl-2 family proteins in regulating mitochondrial dynamics, we carried out a detailed analysis of mitochondria in animals that either lose or have increased activity of *egl-1* and *ced-9*, two Bcl-2 family genes that induce and inhibit apoptosis in *C. elegans*, respectively. Unexpectedly, we found that loss of *egl-1* or *ced-9*, or overexpression of their gene products, had no apparent effect on mitochondrial connectivity or mitochondrial size. Moreover, loss of *ced-9* did not affect the mitochondrial morphology observed in a *drp-1* mutant, in which mitochondrial fusion occurs but mitochondrial fission is defective, or in a *fzo-1* mutant, in which mitochondrial fission occurs but mitochondrial fusion is restricted, suggesting that *ced-9* is not required for either the mitochondrial fission or fusion process in *C. elegans*. Taken together, our results argue against an evolutionarily conserved role for Bcl-2 proteins in regulating mitochondrial fission and fusion.

Results

Mitochondrial Morphogenesis Is Not Affected in *egl-1(lf)* or *ced-9(lf)* Mutants

Recently, the *C. elegans* proapoptotic BH3-only Bcl-2 protein EGL-1 has been implicated in promoting mitochondria fission during apoptosis [1]. In addition, the *C. elegans* antiapoptotic Bcl-2 protein CED-9 was shown to mediate mitochondria fission during apoptosis in one study [1] but was found to promote mitochondria fusion in healthy cells in another [2], calling into question of the exact physiological roles of *C. elegans* Bcl-2 family proteins in regulating mitochondria dynamics. To address the critical issue of whether Bcl-2 proteins regulate normal mitochondrial fission or fusion process in *C. elegans*, we carried out a comprehensive analysis of mitochondria morphology and structure in animals that either lose or have increased activity of *egl-1* or *ced-9*. First, we visualized mitochondria in early *C. elegans* embryos that were stained with the mitochondria-specific dye tetramethylrhodamine ethyl ester (TMRE); the large blastomere size in early embryos permits clear visualization of the mitochondrial network. In N2 (wild-type) animals, in which mitochondrial fission and fusion processes are balanced, mitochondria appeared as a large network, evenly distributed through out each cell (Figure 1A) [1, 3–7]. In *drp-1(tm1108)* mutant animals, which are null for the DRP-1 protein expression and defective in mitochondrial fission [7], mitochondria appeared as highly connected clusters and asymmetrically distributed in individual blastomeres (Figure 1B), which results from ongoing mitochondrial fusion in the absence of mitochondrial fission [6]. In contrast, in *fzo-1(tm1133)* animals, which harbor a deletion in the *fzo-1* gene and in which mitochondrial fusion is compromised but mitochondrial fission continues [7], the mitochondrial network was disrupted into highly fragmented, punctiform organelles (Figure 1C). Thus, a defect in either the mitochondrial fission or fusion process is clearly identifiable in this assay.

Mitochondria in *egl-1(n3082)* animals, which carry a strong loss-of-function (*lf*) mutation in *egl-1*, appeared undistinguishable from those in wild-type animals (Figure 1D), although somatic programmed cell death is abolished in these animals [8]. Similarly, the mitochondrial network appeared unaffected in *ced-9(n1950 gf)* animals (Figure 1E), which carry a gain-of-function (*gf*) mutation (a G169E substitution) in the *ced-9* gene that prevents EGL-1 from binding to CED-9 [9, 10] and thus blocks *C. elegans* programmed cell death [11]. We also analyzed mitochondria morphology in two *ced-9(lf)* mutants: *ced-9(n1653ts)* and *ced-9(n2812)*. The *n1653* mutation causes a Y149N substitution in CED-9 that reduces its association with CED-4 at the restrictive temperature (25°C) and compromises its apoptosis inhibitory activity [12], leading to ectopic apoptosis. *n2812* is an early nonsense mutation in the *ced-9* gene [13] and a putative null allele that abolishes expression of *ced-9* in *C. elegans* [14]. *ced-9(n2812)* animals are embryonic lethal as a result of excessive apoptosis but can be maintained and analyzed in the *ced-3(lf)* or *ced-4(lf)* mutant background, which blocks apoptosis [11]. As shown in Figures 1F–1H, we observed no significant difference in mitochondrial morphology in *ced-9(n1653ts)*, *ced-4(n1162) ced-9(n2812)*, or *ced-9(n2812); ced-3(n717)* embryos compared to that in N2 embryos or that in *ced-3(n717)* or *ced-4(n1162)* embryos or *ced-9(n1653ts)* embryos at the permissive temperature (Figure S1 available online). We quantified the connectivity of mitochondria in N2, *drp-1(tm1108), fzo-1(tm1133), egl-1(n3082)*, and *ced-9(n2812); ced-3(n717)* blastomeres by generating line intensity plots and calculating the frequency of major TMRE fluorescent spikes (Figure S2; method described in Supplemental Experimental Procedures). In N2 blastomeres, TMRE fluorescent signals varied in frequency, with an average of 0.49 fluorescent spikes/μm (Figure S2). TMRE fluorescent signals were very broad and of low spike frequency in *drp-1(tm1108)* blastomeres (average frequency of 0.16 fluorescent spikes/μm; Figure S2), consistent with large

*Correspondence: breckenridge.david@gmail.com (D.G.B.), ding.xue@colorado.edu (D.X.)
[3]These authors contributed equally to this work

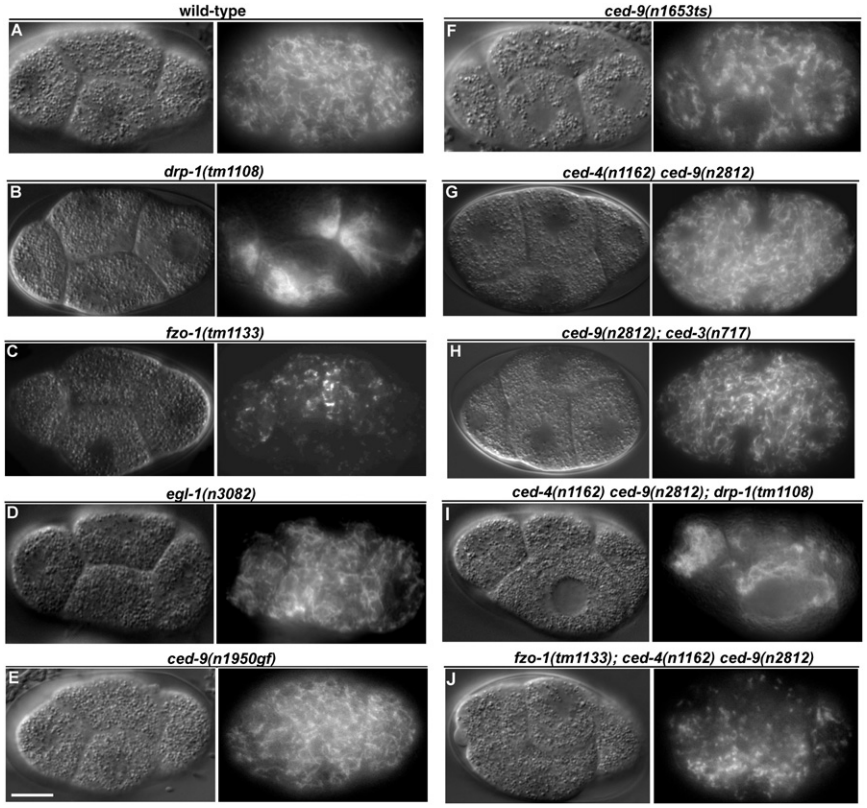

Figure 1. The Mitochondrial Network Is Altered in *fzo-1* and *drp-1* Mutants but Unaffected by Mutations in *egl-1* and *ced-9*

Animals were stained with tetramethylrhodamine ethyl ester (TMRE), a mitochondrial-specific dye, and blastomeres at the four-cell embryonic stage were imaged. Embryos were visualized by differential interference contrast (DIC, left) and rhodamine fluorescence (right) microscopy. Representative images are shown. Compared to wild-type embryos (A), *drp-1(tm1108)* embryos (B) have a highly connected mitochondrial network, whereas mitochondria appeared highly fragmented in *fzo-1(tm1133)* embryos (C). Mitochondria in *egl-1(n3082)* (D), *ced-9(n1950 gf)* (E), *ced-9(n1653ts)* at the restrictive temperature (F), *ced-4(n1162) ced-9(n2812)* (G), and *ced-9(n2812); ced-3(n717)* (H) embryos were indistinguishable from those observed in wild-type embryos. Loss of *ced-9* has no effect on the mitochondria morphology in *drp-1(tm1108)* or *fzo-1(tm1133)* animals. The mitochondrial network in the *ced-4(n1162) ced-9(n2812); drp-1(tm1108)* embryo (I) and in the *fzo-1(tm1133); ced-4(n1162) ced-9(n2812)* embryo (J) is similar to that seen in *drp-1(tm1108)* embryos (B) and *fzo-1(tm1133)* embryos (C), respectively. The scale bar represents 10 μm.

clumps of mitochondria asymmetrically distributed within cells. In contrast, *fzo-1(tm1133)* embryos displayed high frequency of TMRE signal spikes, averaging 2.29 spikes/μm, delineating punctiform mitochondria evenly distributed throughout the cells (Figure S2). The frequency of TMRE signal spikes in *egl-1(n3082), ced-9(n1950 gf)* or *ced-9(n2812); ced-3(n717)* blastomeres was similar to that of N2 animals (an average frequency of 0.44 spikes/μm and 0.48 spikes/μm in *egl-1(n3082)* and *ced-9(n2812); ced-3(n717)* blastomeres; Figure S2). Taken together, these results suggest that loss of *egl-1* or *ced-9* function does not affect mitochondria dynamics and morphology in *C. elegans*.

Of note, a recent report showed that mitochondria appeared highly fragmented in *ced-9(n1653ts)* embryos at the restrictive temperature [2]. However, in that study, embryos were examined at a later stage of development and the mitochondrial fragmentation observed could have been the result of widespread ectopic apoptosis [1, 7], rather than a requirement for *ced-9* to maintain the integrity of the mitochondrial network. Importantly, CED-9 protein is ubiquitously expressed in embryos as early as the two-cell stage [14]. If CED-9 is required to maintain normal mitochondrial networks, its role should be uncovered in early embryos. The expression pattern of EGL-1 is not well understood, but *egl-1* transcription has been shown to be upregulated in several cells destined to die [15]. Nonetheless, our results suggest that the activity of *egl-1* is not required for normal mitochondrial morphogenesis.

We carried out electron microscopy (EM) analysis to confirm the TMRE staining results in Figure 1 and to investigate whether *egl-1* or *ced-9* might play subtle roles in regulating mitochondrial dynamics. In 2D images of EM sections from N2 embryos, mitochondria appeared in a variety of shapes and sizes, ranging from small spherical organelles to longer dumbbell-shaped organelles (Figure 2A), and with a mean longitudinal length of 0.94 μm (Figure 2F). As expected, mitochondria in *drp-1(tm1108)* embryos were very long, with fewer individual mitochondria observed in each cell (Figure S3A) and a mean mitochondrial length of 2.28 μm (Figure 2F) [7]. *fzo-1(tm1133)* embryos displayed only small and spherical mitochondria, with a mean mitochondrial length of 0.38 μm (Figure S3B and Figure 2F). However, mitochondria in *egl-1 (n3082)*, *ced-9(n1950 gf)*, *ced-9(n1653ts)*, and *ced-9(n2812); ced-3(n717)* embryos appeared similar to those observed in N2 embryos and in all cases had mean longitudinal mitochondrial lengths that were not significantly different from those of N2 animals (Figures 2B–2E). Mitochondria in the germline, gut, and muscle cells of adult *egl-1(lf)*, *ced-9(lf); ced-3(lf)*, or *ced-9(gf)* mutants also appeared to be normal (data not shown). The mitochondrial morphology in N2, *drp-1(tm1108)*, *fzo-1(tm1133)*, *egl-1(n3082)*, and *ced-9(n2812); ced-3(n717)* animals was confirmed by serial EM sectioning and 3D reconstruction from the serial images (Figure 3 and Figure S4). Again, mitochondria in N2, *egl-1(n2812)*, and *ced-9(n2812); ced-3(n717)* animals varied in shape and size and were evenly distributed throughout the cell. In contrast, mitochondria in *drp-1(tm1108)* embryos were long, highly interconnected, and clustered around the nucleus, whereas mitochondria in *fzo-1(tm1133)* embryos were small, puntiform, and evenly distributed. Altogether, these results confirm that *egl-1* and *ced-9* do not have a detectable role in regulating mitochondrial fission or fusion in *C. elegans.*

ced-9 Does Not Promote *drp-1*-Dependent Mitochondrial Fission or *fzo-1*-Dependent Mitochondrial Fusion

If CED-9 somehow has both profission and profusion activities as previously reported [1, 2], it is conceivable that loss of *ced-9*

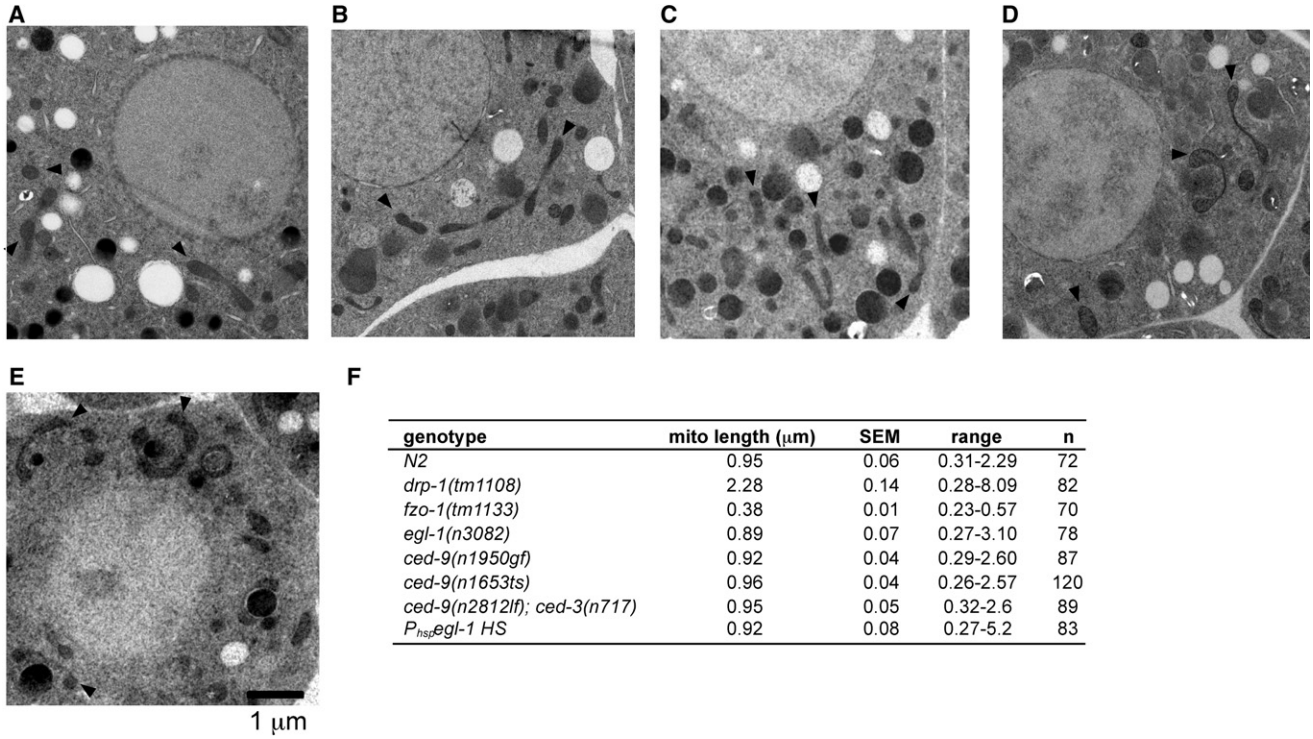

genotype	mito length (μm)	SEM	range	n
N2	0.95	0.06	0.31-2.29	72
drp-1(tm1108)	2.28	0.14	0.28-8.09	82
fzo-1(tm1133)	0.38	0.01	0.23-0.57	70
egl-1(n3082)	0.89	0.07	0.27-3.10	78
ced-9(n1950gf)	0.92	0.04	0.29-2.60	87
ced-9(n1653ts)	0.96	0.04	0.26-2.57	120
ced-9(n2812lf); ced-3(n717)	0.95	0.05	0.32-2.6	89
P_{hsp}*egl-1 HS*	0.92	0.08	0.27-5.2	83

Figure 2. Electron Microscopy Analysis of Mitochondria Morphology in *egl-1* and *ced-9* Mutants

Representative electron micrographs of embryos from the following strains are shown: N2 (A), *egl-1(n3082)* (B), *ced-9(n1950 gf)* (C), *ced-9(n1653ts)* at the restrictive temperature (D), and *ced-9(n2812); ced-3(n717)* (E). The scale bar represents 1 μm. Arrows indicate representative mitochondria. (F) shows the quantification of the mean mitochondrial length. Randomly selected mitochondria from electron micrographs were measured along their longitudinal axis. SEM, standard error of the mean. n, the number of mitochondria scored.

in *C. elegans* would yield no net effect on the mitochondrial network. To address this possibility, we examined the effect of a *ced-9(lf)* mutation on the mitochondrial morphologies in *drp-1(tm1108)* and *fzo-1(tm1133)* mutant backgrounds, where mitochondrial fusion or fission occurs in isolation, respectively [5]. Mitochondria in *fzo-1(tm1133); ced-4(n1162) ced-9(n2812)* triple-mutant embryos appeared highly fragmented and indistinguishable from mitochondria in *fzo-1(tm1133); ced-4(n1162)* or *fzo-1(tm1133)* embryos (Figures 1C and 1J and data not shown). On the other hand, mitochondria in *ced-4(n1162) ced-9(n2812); drp-1(tm1108)* triple mutants were highly connected and asymmetrically distributed in the cells, just as was observed in *ced-4(n1162); drp-1(tm1108)* and *drp-1(tm1108)* animals (Figures 1B and 1I and data not shown). Therefore, in a physiological setting (i.e., where *ced-9*, *drp-1*, and *fzo-1* are not overexpressed), loss of *ced-9* has no discernable effect on either *drp-1*-dependent mitochondrial fission or *fzo-1*-dependent mitochondrial fusion. In comparison, *drp-1(tm1108)* completely suppresses the highly fragmented mitochondria phenotype caused by the *fzo-1(tm1133)* mutation [7], indicating that *drp-1* is required for the mitochondrial fragmentation observed in *fzo-1* mutants.

Overexpression of CED-9 or EGL-1 Does Not Promote Mitochondrial Fission or Fusion

Although *egl-1* and *ced-9* are not required for mitochondrial fission or fusion in normal cells, they might directly affect one of these processes during apoptosis [1]. Therefore, we examined whether overexpression of either EGL-1 or CED-9 could affect mitochondrial morphology in *C. elegans*, in comparison with their activities in inducing or inhibiting apoptosis. We generated animals carrying an integrated transgene of *egl-1* or *ced-9* under the control of heat-shock promoters (P_{hsp}*egl-1* and P_{hsp}*ced-9*, respectively) and examined the mitochondrial network in young embryos before and after heat-shock treatment. Because overexpression of EGL-1 potently induces ectopic apoptosis in *C. elegans* [8] and overexpression of CED-9 strongly inhibits normal programmed cell death [13], we quantified the effect of induced overexpression of EGL-1 and CED-9 on cell death by counting the number of cell corpses in heat-treated P_{hsp}*egl-1* and P_{hsp}*ced-9* embryos and the number of cells that should die but inappropriately survived in the anterior pharynx of larvae that hatched from the heat-treated P_{hsp}*ced-9* embryos. Heat-shock treatment of P_{hsp}*egl-1* embryos resulted in the appearance of over 40 cell corpses by the comma stage of embryonic development (Figure 4A) and ultimately caused growth arrest and death of all embryos prior to hatching (data not shown). In contrast, heat-shock treatment of P_{hsp}*ced-9* animals greatly reduced the number of cell corpses in embryos (Figure 4A) and caused on average the survival of over nine extra cells in the anterior pharynx of the resulting larvae (Figure 4B). These results demonstrate that induced global expression of EGL-1 and CED-9 potently promotes or inhibits apoptosis in P_{hsp}*egl-1* and P_{hsp}*ced-9* animals, respectively. However, we did not observe an obvious change in mitochondrial morphology in P_{hsp}*egl-1* or P_{hsp}*ced-9* embryos after the heat-shock treatment (Figure 4C). In contrast, *drp-1(tm1108)* or *fzo-1(tm1133)* embryos at the same developmental stage

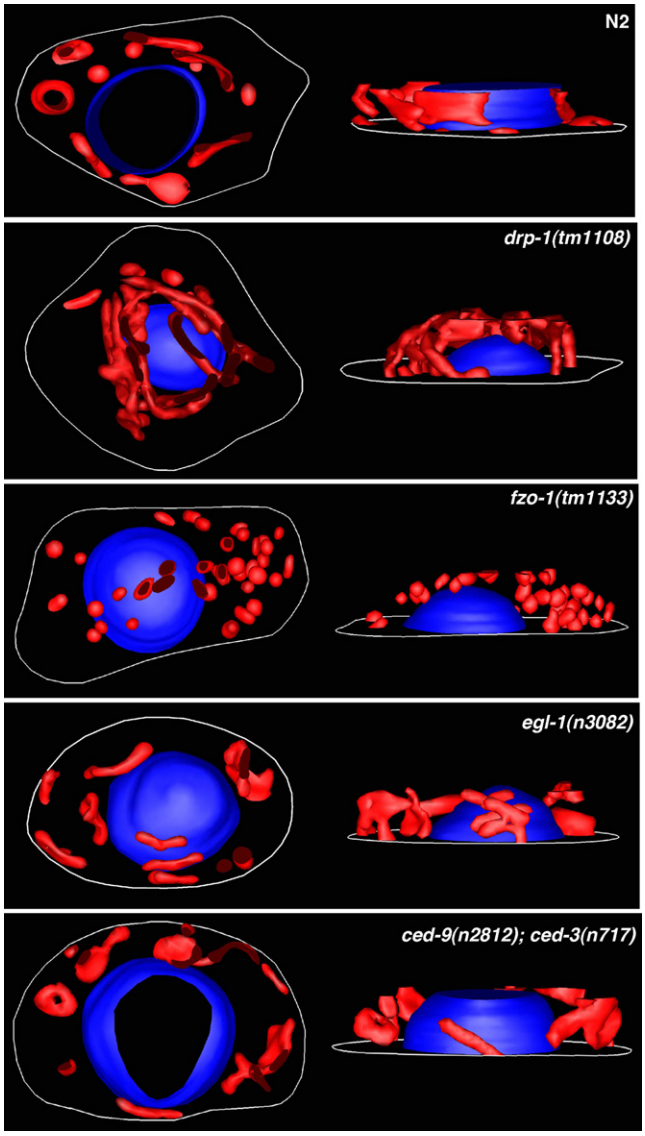

Figure 3. 3D Mitochondria Images Reconstructed from Serial Electron Micrographs

3D models of mitochondria (red) in various mutant embryos were generated from stacks consisting of 15~20 serial electron micrographs (10,000×) of 80-nm-thick sections (see Experimental Procedures for detail). In each panel, the top-down view (left) and side view (right) of the cell are shown. Mitochondria in the *drp-1(tm1108)* mutant are interconnected to form a large network, whereas mitochondria in the *fzo-1(tm1133)* mutant are highly fragmented and spherical. No obvious difference is seen in mitochondria organization and architecture among N2, *egl-1(n3082)*, and *ced-9(n2812); ced-3(n717)* embryos. Nuclei (blue) and cell outlines (white) are also shown.

showed clear signs of mitochondrial clustering and mitochondrial fragmentation, respectively (Figure S5). Analysis of EM micrographs of heat-treated P_{hsp}*egl-1* embryos revealed that in most cells mitochondria appeared to be normal (Figure 4D) and that the mean mitochondrial length remained at 0.92 μm, similar to what was observed in N2 animals (Figure 2F). Highly fragmented and spherical mitochondria were observed in cell corpses of P_{hsp}*egl-1* embryos (Figure 4E), suggesting that mitochondria eventually fragment in dying cells, probably as a secondary event of apoptosis. Consistent with this, we did not observe evidence of widespread mitochondrial fragmentation or ectopic apoptosis when EGL-1 was overexpressed in a *ced-3(lf)* background, even when animals were observed up to 5 hr after heat-shock treatment (Figure S6; data now shown). Therefore, elevated levels of EGL-1 and CED-9 proteins do not appear to directly promote either mitochondrial fission or fusion in *C. elegans.* However, our results do not rule out the possibility that EGL-1 may play a role in promoting mitochondria fragmentation in normally dying cells. Of note, it was reported that ectopic *egl-1* expression (using a similar P_{hsp}*egl-1*construct) induced widespread mitochondrial fission, independent of *ced-3* [1]. The reason for the discrepancy between that study and ours is currently unclear.

Discussion

Although several recent reports have suggested a connection between Bcl-2 proteins and the mitochondrial fission or fusion process [1, 2, 16–18], we did not find an obvious requirement for *egl-1* or *ced-9* in regulating either process in *C. elegans*. Analysis of strong loss-of-function *egl-1* and *ced-9* mutants and a gain-of-function *ced-9* mutant, which either are defective in apoptosis or contain excessive cell deaths, revealed no detectable difference in the mitochondrial network when observed in live animals stained with mitochondria-specific dye, in high-magnification EM sections, or in 3D models reconstructed from serial EM sections. Moreover, *ced-9* does not affect either *drp-1*-dependent mitochondrial fission or *fzo-1*-dependent mitochondrial fusion in vivo (Figures 1B, 1C, 1I, and 1J). These findings disagree with two recent reports that proposed a role for EGL-1 and CED-9 in regulating mitochondrial dynamics in *C. elegans* [1, 2]. In one report, overexpression of EGL-1 was shown to induce mitochondrial fragmentation, independent of *ced-3*, and mitochondrial fission induced by ectopic *drp-1* expression was blocked by both *ced-9(n1950 gf)* and *ced-9(n2812lf)* mutations [1]. However, we did not observe widespread mitochondrial fragmentation after EGL-1 induction (Figure 4) and loss of *ced-9* does not affect mitochondria fission or fusion on its own or affect *drp-1*-dependent mitochondrial fission when examined in a physiological context (i.e., in the *fzo-1* mutant background when *drp-1* was not overexpressed) (Figures 1C and 1J). Mitochondria are fragmented in cell corpses after EGL-1 induction, but this is probably the result of a downstream caspase-dependent apoptotic process [7] rather than a process that is regulated by EGL-1 or CED-9 to activate apoptosis. Indeed, we did not detect any obvious cell-death defect in the strong loss-of-function *drp-1(tm1108)* mutant, in which mitochondria are highly fused, or in animals deficient in *fzo-1* or *eat-3*, in which mitochondria are highly fragmented [7], indicating that the mitochondria fusion or fission process does not play a role in apoptosis activation. Similarly, we found that overexpression of CED-9 in *C. elegans* does not induce mitochondrial fission or fusion, although its overexpression was reported to cause excessive mitochondrial fusion in cultured mammalian cells [2]. Therefore, in mammalian cells CED-9 may target proteins or signaling pathways that don't exist in the worm. Taken together, our findings indicate that EGL-1 and CED-9 do not have a discernable role in promoting either mitochondrial fission or fusion in *C. elegans* and challenge the hypothesis that regulation of mitochondrial morphogenesis is an evolutionarily conserved feature of Bcl-2 proteins [2].

In mammals, overexpression of Bcl-xL can induce both mitochondrial fission and fusion depending on its level of expression [2, 17] and can increase mitochondrial biomass

A

	Number of Cell Corpses					
	No Heat shock			Heat shock		
genotype	mean	SEM	range	mean	SEM	range
N2	9.77	0.5	7-13	10.4	0.6	7-13
P_{hsp}*ced-9*	8.9	0.5	6-12	0.6	0.2	0-3
P_{hsp}*egl-1*	10.6	0.5	6-14	40.7	2.8	25-61

B

	Number of Extra Cells					
	No Heat shock			Heat shock		
genotype	mean	SEM	range	mean	SEM	range
N2	0.1	0.1	0-1	0.1	0.1	0-1
P_{hsp}*ced-9*	0.2	0.1	0-1	9.4	0.45	6-12

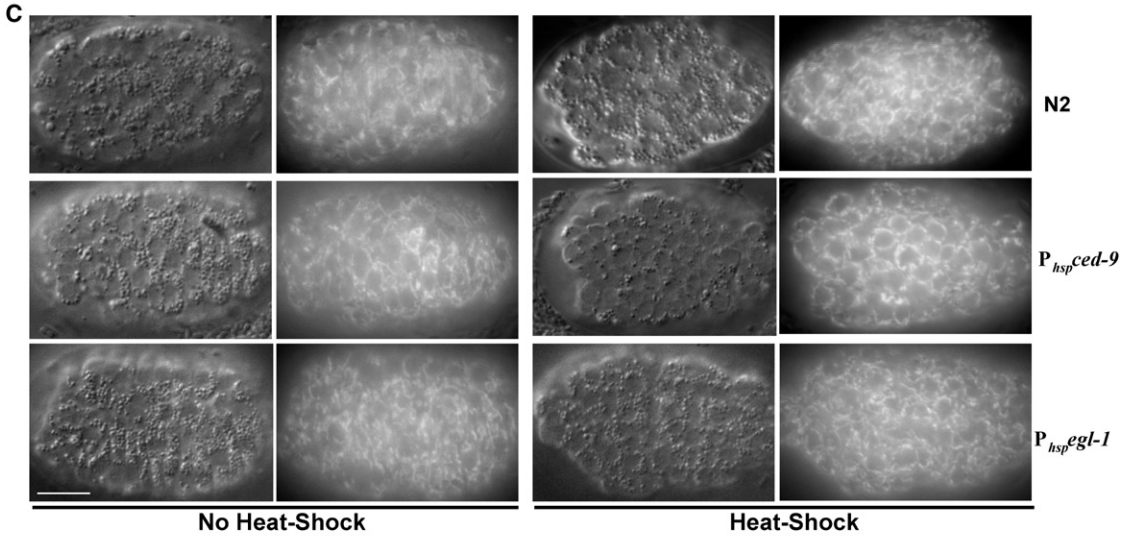

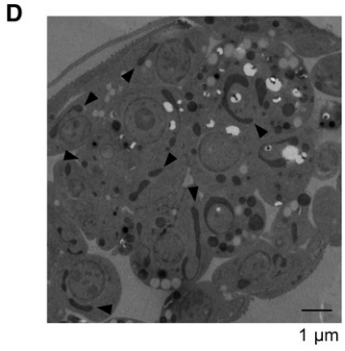

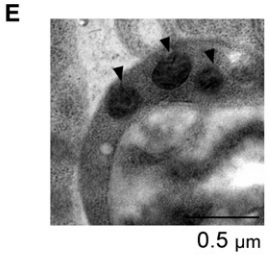

Figure 4. Overexpression of EGL-1 or CED-9 Affects Programmed Cell Death in *C. elegans* but Does Not Obviously Affect Mitochondrial Morphogenesis

(A) N2, P_{hsp}*egl-1* (*smIs82*), or P_{hsp}*ced-9* (*smIs157*) embryos were treated with heat-shock (right) or left untreated (left), and the number of cell corpses in the head region of 1.5-fold-stage embryos was scored 2 hr after heat-shock treatment.

(B) Embryos of the indicated genotypes were treated with heat-shock (right) or left untreated (left) and allowed to hatch into L4 larvae, at which point the number of extra cells that inappropriately survived in the anterior pharynx was scored. Twenty animals were scored in both (A) and (B).

(C) N2, P_{hsp}*egl-1*, or P_{hsp}*ced-9* embryos were stained with TMRE and either treated with heat-shock (right) or left untreated (left) and visualized by differential interference CONTRAST (DIC) and rhodamine fluorescence microscopy. Mitochondria in heat-shock-treated P_{hsp}*egl-1* or P_{hsp}*ced-9* embryos were indistinguishable from those observed in untreated embryos and wild-type embryos. The scale bar represents 10 μm.

(D) An EM micrograph of a heat-shock-treated P_{hsp}*egl-1* embryo. Arrows indicate several mitochondria of various shapes and sizes.

(E) Mitochondria in a cell corpse of a heat-shock-treated P_{hsp}*egl-1* embryo are fragmented as a result of apoptosis. SEM, standard error of the mean.

[17], whereas overexpression of Bcl-2 promotes mitochondrial fusion [2] and overexpression of Bax induces mitochondrial fission and apoptosis [16]. Paradoxically, Bax and Bak are also reported to be important for mitochondrial fusion in healthy cells [18], raising an interesting question of how mammalian Bcl-2 proteins achieve opposing functions in mitochondria dynamics. Bcl-2 proteins might affect mitochondria fusion or fission in mammals by interacting with the mitochondrial fusion machinery, given that Bcl-xL was shown to interact with Mfn2 [2] and Bax/Bak were found to be required for Mfn2 to form discrete foci in the outer mitochondrial membrane [18]. Therefore, it appears that mammalian Bcl-2

proteins may have evolved a role to directly or indirectly regulate mitochondrial fission and fusion, and such a role does not appear to exist in their worm counterparts. Further analysis of mitochondria dynamics under physiological settings will be critical to understand the roles and mechanisms of mammalian Bcl-2 proteins in regulating mitochondria fusion and fission.

Supplemental Data

Supplemental Data include Supplemental Experimental Procedures and six figures and can be found with this article online at http://www.cell.com/current-biology/supplemental/S0960-9822(09)00825-2.

Acknowledgments

We thank *Caenorhabditis* Genetics Center for strains and Tom Giddings for assistance with EM operation. This research was supported in part by fellowships from the Jane Coffins Child Memorial Fund for Medical Research and the Canadian Institutes of Health Research (D.G.B), start-up funds from the University of Florida (B.H.K), the Burroughs Wellcome Fund Career Award (D.X.), and the National Institutes of Health R01 GM059083 and GM079097 grants (D.X.).

Received: August 1, 2008
Revised: March 5, 2009
Accepted: March 5, 2009
Published online: March 26, 2009

References

1. Jagasia, R., Grote, P., Westermann, B., and Conradt, B. (2005). DRP-1-mediated mitochondrial fragmentation during EGL-1-induced cell death in *C. elegans*. Nature *433*, 754–760.
2. Delivani, P., Adrain, C., Taylor, R.C., Duriez, P.J., and Martin, S.J. (2006). Role for CED-9 and EGL-1 as regulators of mitochondrial fission and fusion dynamics. Mol. Cell *21*, 761–773.
3. Ichishita, R., Tanaka, K., Sugiura, Y., Sayano, T., Mihara, K., and Oka, T. (2008). An RNAi screen for mitochondrial proteins required to maintain the morphology of the organelle in *C. elegans*. J. Biochem. *143*, 449–454.
4. Chan, D.C. (2006). Mitochondrial fusion and fission in mammals. Annu. Rev. Cell Dev. Biol. *22*, 79–99.
5. Okamoto, K., and Shaw, J.M. (2005). Mitochondrial morphology and dynamics in yeast and multicellular eukaryotes. Annu. Rev. Genet. *39*, 503–536.
6. Labrousse, A.M., Zappaterra, M.D., Rube, D.A., and van der Bliek, A.M. (1999). *C. elegans* dynamin-related protein DRP-1 controls severing of the mitochondrial outer membrane. Mol. Cell *4*, 815–826.
7. Breckenridge, D.G., Kang, B.-H., Kokel, D.K., Mitani, S., Staehelin, L.A., and Xue, D. (2008). *Caenorhabditis elegans drp-1* and *fis-2* regulate distinct cell death execution pathways downstream of *ced-3* and independent of *ced-9*. Mol. Cell *31*, 586–597.
8. Conradt, B., and Horvitz, H.R. (1998). The *C. elegans* protein EGL-1 is required for programmed cell death and interacts with the Bcl-2-like protein CED-9. Cell *93*, 519–529.
9. Hengartner, M.O., and Horvitz, H.R. (1994). Activation of *C. elegans* cell death protein CED-9 by an amino-acid substitution in a domain conserved in Bcl-2. Nature *369*, 318–320.
10. Parrish, J., Metters, H., Chen, L., and Xue, D. (2000). Demonstration of the in vivo interaction of key cell death regulators by structure-based design of second-site suppressors. Proc. Natl. Acad. Sci. USA *97*, 11916–11921.
11. Hengartner, M.O., Ellis, R.E., and Horvitz, H.R. (1992). *Caenorhabditis elegans* gene ced-9 protects cells from programmed cell death. Nature *356*, 494–499.
12. Spector, M.S., Desnoyers, S., Hoeppner, D.J., and Hengartner, M.O. (1997). Interaction between the *C. elegans* cell-death regulators CED-9 and CED-4. Nature *385*, 653–656.
13. Hengartner, M.O., and Horvitz, H.R. (1994). *C. elegans* cell survival gene *ced-9* encodes a functional homolog of the mammalian proto-oncogene bcl-2. Cell *76*, 665–676.
14. Chen, F., Hersh, B.M., Conradt, B., Zhou, Z., Riemer, D., Gruenbaum, Y., and Horvitz, H.R. (2000). Translocation of *C. elegans* CED-4 to nuclear membranes during programmed cell death. Science *287*, 1485–1489.
15. Peden, E., Killian, D., and Xue, D. (2008). Cell death specification in *C. elegans*. Cell Cycle *7*, 2479–2484.
16. Karbowski, M., Lee, Y.J., Gaume, B., Jeong, S.Y., Frank, S., Nechushtan, A., Santel, A., Fuller, M., Smith, C.L., and Youle, R.J. (2002). Spatial and temporal association of Bax with mitochondrial fission sites, Drp1, and Mfn2 during apoptosis. J. Cell Biol. *159*, 931–938.
17. Berman, S.B., Chen, Y.-B., Qi, B., McCaffery, J.M., Rucker, E.B., Goebbels, S., Nave, K.A., Arnold, B.A., Jonas, E.A., Pineda, F.J., and Hardwick, M.J. (2009). Bcl-xL increases mitochondrial fission, fusion, and biomass in neurons. J. Cell Biol. *184*, 707–719.
18. Karbowski, M., Norris, K.L., Cleland, M.M., Jeong, S.Y., and Youle, R.J. (2006). Role of Bax and Bak in mitochondrial morphogenesis. Nature *443*, 658–662.

Supplemental Data

Bcl-2 Proteins EGL-1 and CED-9 Do Not Regulate Mitochondrial Fission or Fusion in *Caenorhabditis elegans*

David G. Breckenridge, Byung-Ho Kang, and Ding Xue

Supplemental Experimental Procedures

Strains and culture conditions. Strains of *C. elegans* were maintained at 20°C using standard protocols [1], unless otherwise noted. N2 was the wild type stain. Alleles of *egl-1*, *ced-9*, *ced-4, ced-3; drp-1 and fzo-1* used in this study have been described previously [2] or are described on wormbase. All strains were backcrossed with *N2* animals 5-10 times prior to analysis.

Counting of extra cells. The number of extra surviving cells in the anterior pharynx of L4 larvae was determined as described previously [3, 4]. Statistical analysis was preformed using a Microsoft Excel 2004 software.

Molecular biology and transgenic animals. P_{hsp}*egl-1* and P_{hsp}*ced-9* were constructed by subcloning the respective full-length cDNAs into the pPD49.78 and pPD49.83 vectors, which harbor the *C. elegans hsp-16.2* and *hsp-16.41* promoters, respectively. Plasmids (25 μg/ml) were injected into N2 animals with pRF4 (25 μg/ml), a dominant *rol-6* construct, as a transgenic marker. Stable transgenic lines of Roller animals were then selected. Integrated lines containing the P_{hsp}*egl-1 and* P_{hsp}*ced-9* constructs (*smIs82* and *smIs157,* respectively) were obtained by irradiating the animals with the corresponding extrachromosomal arrays with gamma rays and screening for progeny with 100% inheritance of the transgene. For the heat-shock experiments, heat-shock treatment of

animals was carried out as previously described [5] and the number of cell corpses in comma stage embryos or number of extra cells in the anterior pharynx of hatched L4 larvae was counted.

Live imaging of *C. elegans* mitochondria and electron microscopy. Labeling of mitochondria with tetramethylrhodamine ethyl ester (TMRE; Molecular Probes) was carried out as previously described [5]. For Figure 1 and Figure 4, embryos were dissected from gravid adults on a 2% agar pad soaked in M9 buffer and visualized using an Axioplan 2 Nomarski Microscope (Carl Zeiss MicroImaging Inc., Thorton, NY, USA) equipped with a SensiCam CCD camera and slidebook 4.0 software (Intelligent Imaging Innovations, Denver, CO, USA). Quantitative analysis of TMRE staining in Figure S2 was preformed using the line intensity application in the Slidebook 4.0 software (Intelligent Imaging Innovations, Inc., Denver). To obtain the spatial frequency of fluorescent signal spikes, which reflect individual mitochondria entities, the number of major fluorescent spikes in each profile was divided by the length of the line (10 μm). For each genotype, the frequency of major fluorescent signal spikes was generated from 40 line intensity plots taken from 40 blastomeres within 10 different embryos. For Figure 5, embryos were heat-shock treated, and then later analyzed after a 2 hour recovery period. For visualization of mitochondria by electron microscopy, adult worms or embryos were mixed with *E. coli* and loaded into type B high-pressure freezing planchettes (Baltec, Tucson, AZ). After cryofixed by Baltec HPM010 high-pressure freezer, the samples were freeze-substituted in anhydrous acetone containing 2% osmium tetroxide at –80^{o}C for 4 days and slowly warmed to room temperature over 48 hours. Infiltration with EPON/Araldite resin (Ted Pella, Reddings, CA), mounting, sectioning, and post-staining

were performed essentially as described [6]. Worms and embryos were observed with a Philips (Hillsboro, OR) CM10 electron microscope operated at 80 kV. Quantification of EM sections in Figure 2 was preformed with Image J software. Mitochondrial length was estimated by measuring the longest longitudinal axis of a mitochondrion. Mitochondria were measured in at least 20 different cells from within at least 10 different embryos of each genotype.

Generation of 3D models of mitochondria. Images of 15~20 consecutive EM sections were collected from embryos inside gravid adults with Hitachi H-7000 transmission electron microscope (Hitachi High Technologies America, Inc., Pleasanton, CA; the operation voltage is 75 kV) equipped with MegaViewIII digital camera (Soft Imaging Solutions Corp, Lakewood, CO). The images were converted into mrc stack files with the Midas image alignment program and newstack command of the IMOD software package (Boulder Laboratory of 3D Electron Microscopy of the Cell, University of Colorado at Boulder). 3D models were generated from the image stacks with the 3dmod program (IMOD software package).

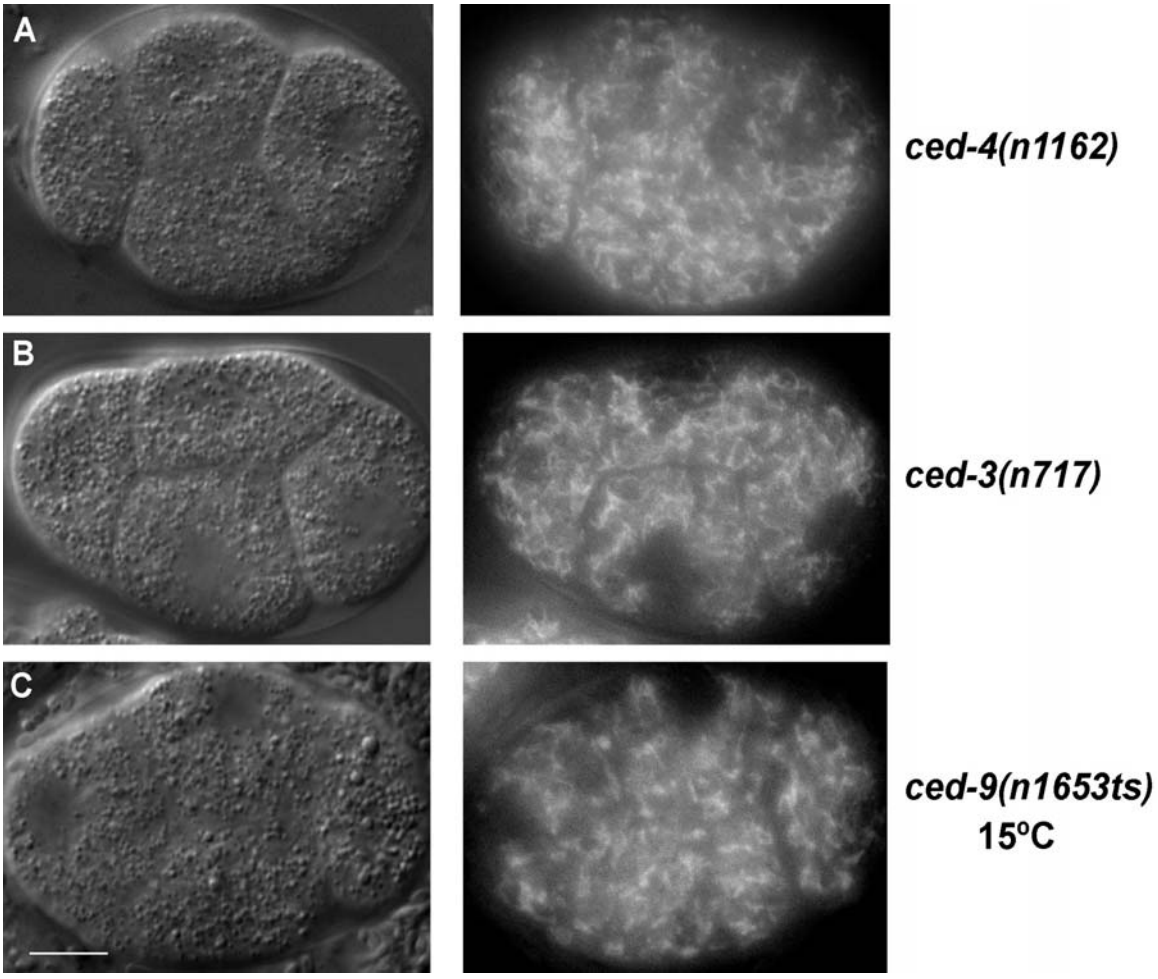

Figure S1. Mitochondrial morphology in *ced-4(n1162)*, *ced-3(n717)*, and *ced-9(n1653ts)* (at the permissive temperature) animals. Animals were stained with tetramethylrhodamine, ethyl ester (TMRE), and blastomeres at the four-cell stage were visualized by Differential Interference Contrast (DIC, left) and rhodamine fluorescence (right) microscopy. (A) *ced-4(n1162)*, (B) *ced-3(n717)*, and (C) *ced-9(n1653ts)* at the permissive temperature (15°C). Scale bar represents 10 μm.

A

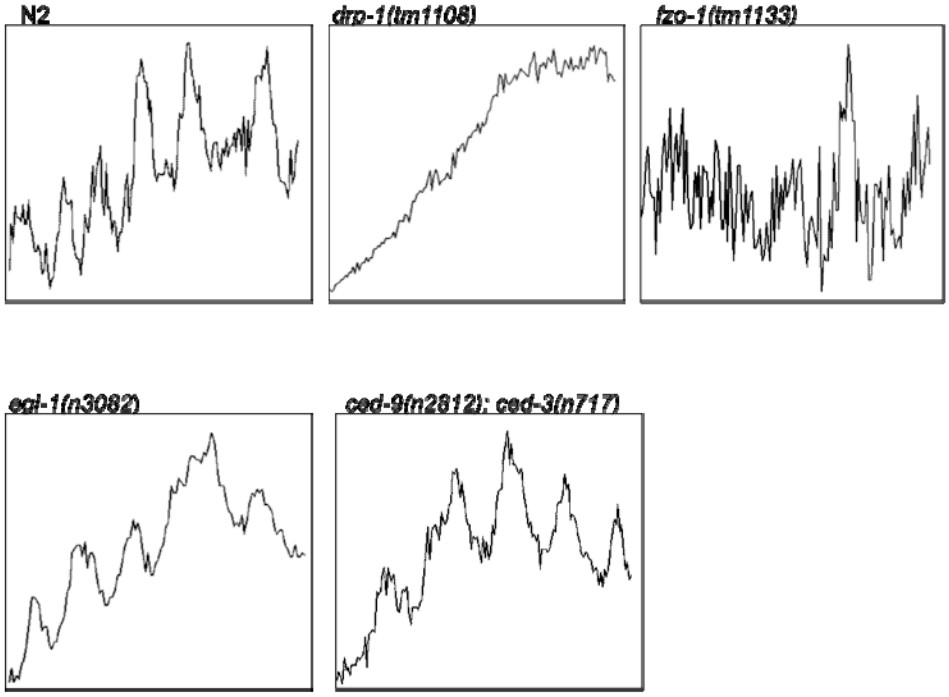

B

genotype	Mean Spike Frequency	SEM	Range	n
N2	0.49	0.03	0.20-0.90	40
drp-1(tm1108)	0.16	0.02	0.10-0.50	40
fzo-1(tm1133)	2.29	0.10	0.70-3.50	40
egl-1(n3082)	0.44	0.03	0.20-0.90	40
ced-9(n2812); ced-3(n717)	0.48	0.03	0.20-0.90	40

Figure S2. Quantification of mitochondrial connectivity in TMRE stained embryos. A) Representative line intensity plots for *N2, drp-1(tm1108), fzo-1(tm1133), egl-1(n3082*), and *ced-9(n2812); ced-3(n717)* blastomeres. Plots were generated by measuring TMRE fluorescence intensity along a randomly chosen 10 μm line. Relative fluorescent intensity is displayed on the Y axis and the distance along the 10 μm line is represented on the X axis. B) Mitochondrial connectivity was quantified by measuring the mean frequency of major fluorescent signal spikes per 10 μm line intensity plot from TRME images of N2*, drp-1(tm1108), fzo-1(tm1133), egl-1(n3082*), and *ced-9(n2812); ced-3(n717)* blastomeres. For each genotype, the average frequency of major fluorescent

signal spikes was generated from 40 line intensity plots taken from 40 blastomeres within 10 different embryos. Two tailed *t* test on mean values: N2 versus *drp-1(tm1108),* P= 3.0e-18; N2 versus *fzo-1(tm1133),* P=1.1e-30; N2 versus *egl-1(n3082),* P=0.5; N2 versus *ced-9(n2812*); *ced-3(n717),* P=0.6.

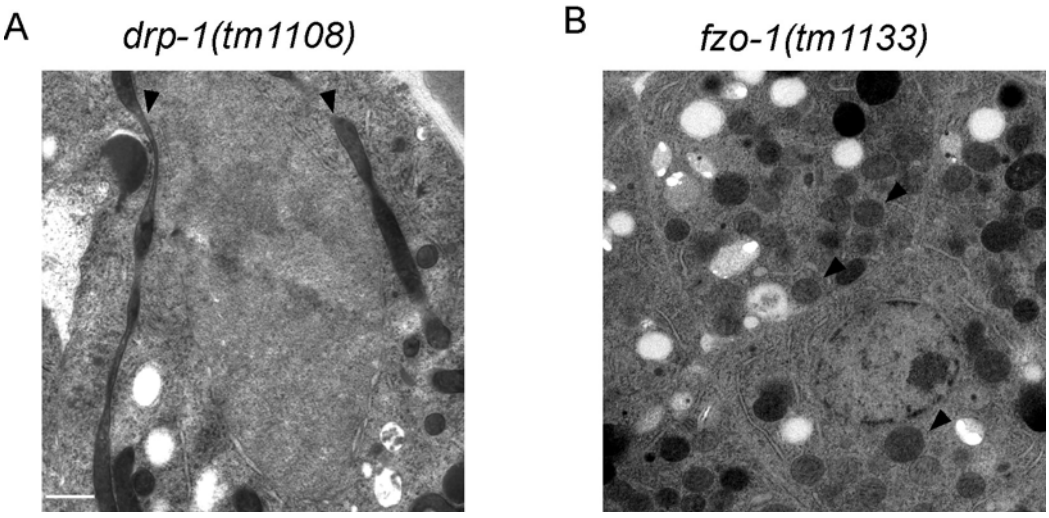

Figure S3. Representative EM micrographs of (A) *drp-1(1108)* and (B) *fzo-1(tm1133)* embryos. Compared to N2 animals (Figure 1) mitochondria were judged to be longer in *drp-1(tm1108)* animals, and small and spherical in *fzo-1(tm1133)* animals. Arrowheads indicate representative mitochondria. Scale bar represents 1 μm.

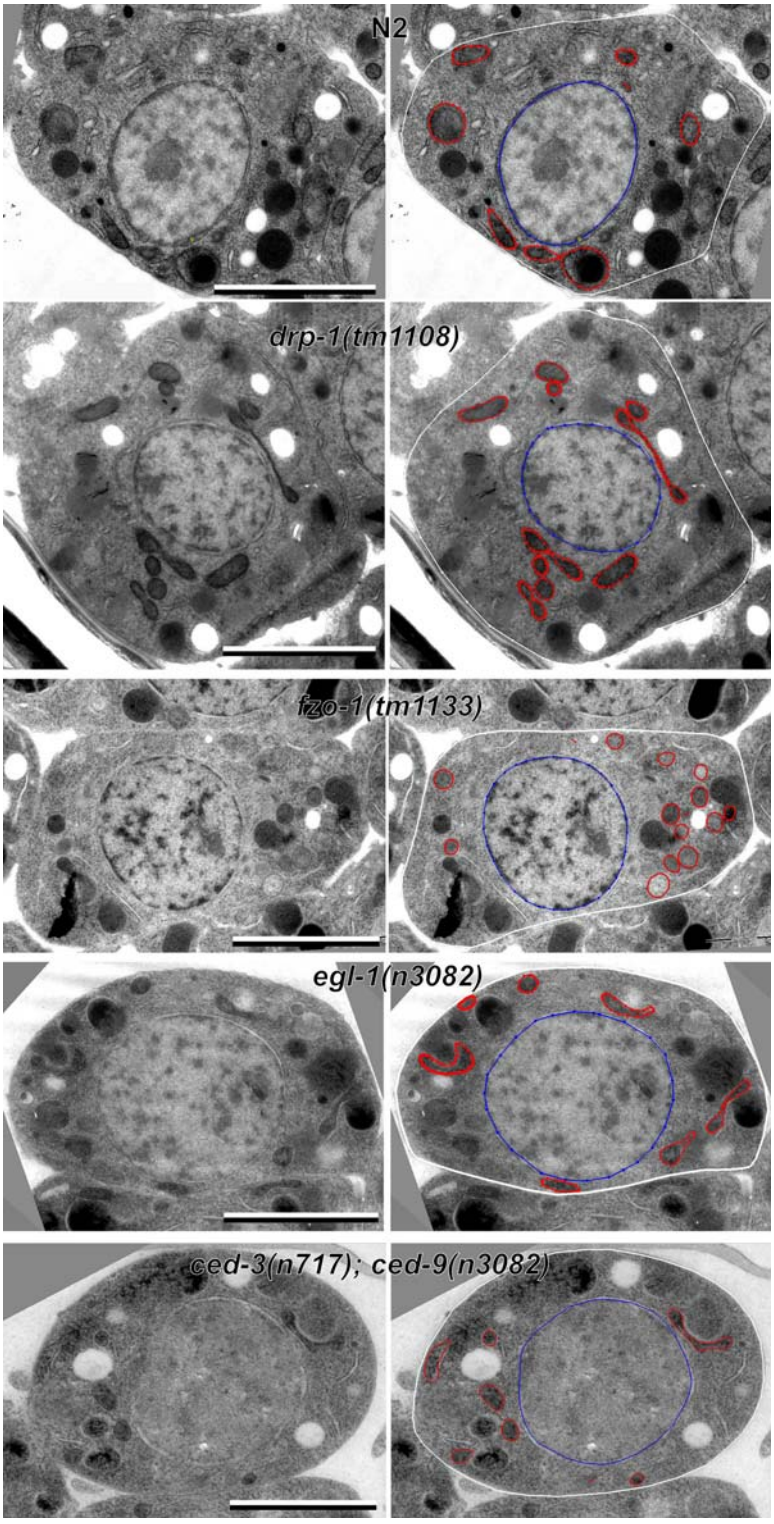
N2
drp-1(tm1108)
fzo-1(tm1133)
egl-1(n3082)
ced-3(n717); ced-9(n3082)

Figure S4. Electron micrographs used for 3D reconstruction. Thin section electron micrographs of *C. elegans* embryos (left) and examples of tracings (red for mitochondria, blue for nuclei, and white for cell outlines) used to generate 3D models in Figure 3 (right) are shown. Scale bars: 2 μm.

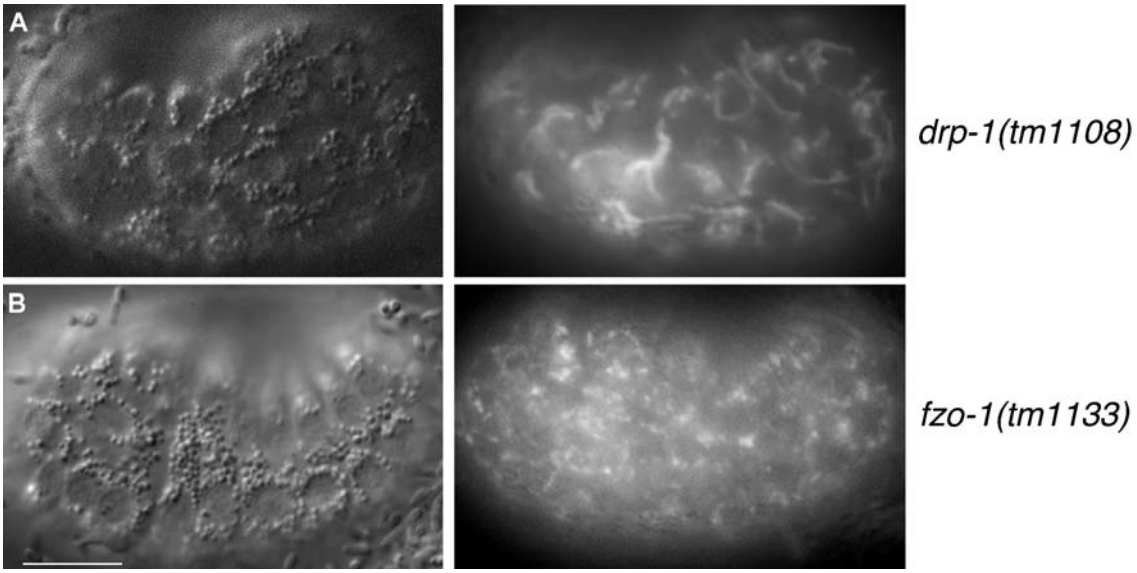

Figure S5. Mitochondrial morphology in *drp-1(tm1108)* and *fzo-1(tm1133)* embryos near the bean stage of development. Animals were stained with tetramethylrhodamine, ethyl ester (TMRE), and visualized by Differential Interference Contrast (DIC, left) and rhodamine fluorescence (right) microscopy. (A) *drp-1(tm1108)*, (B) *fzo-1(tm1133).* Note that mitochondria appear long, clumpy and asymmetrically disturbed within cells in *drp-1(tm1108)* embryos, indicative of unbalanced mitochondrial fusion. Mitochondria appear highly punctate in *fzo-1(tm1133)* embryos, indicative of unbalanced fission. Scale bar represents 10 μm.

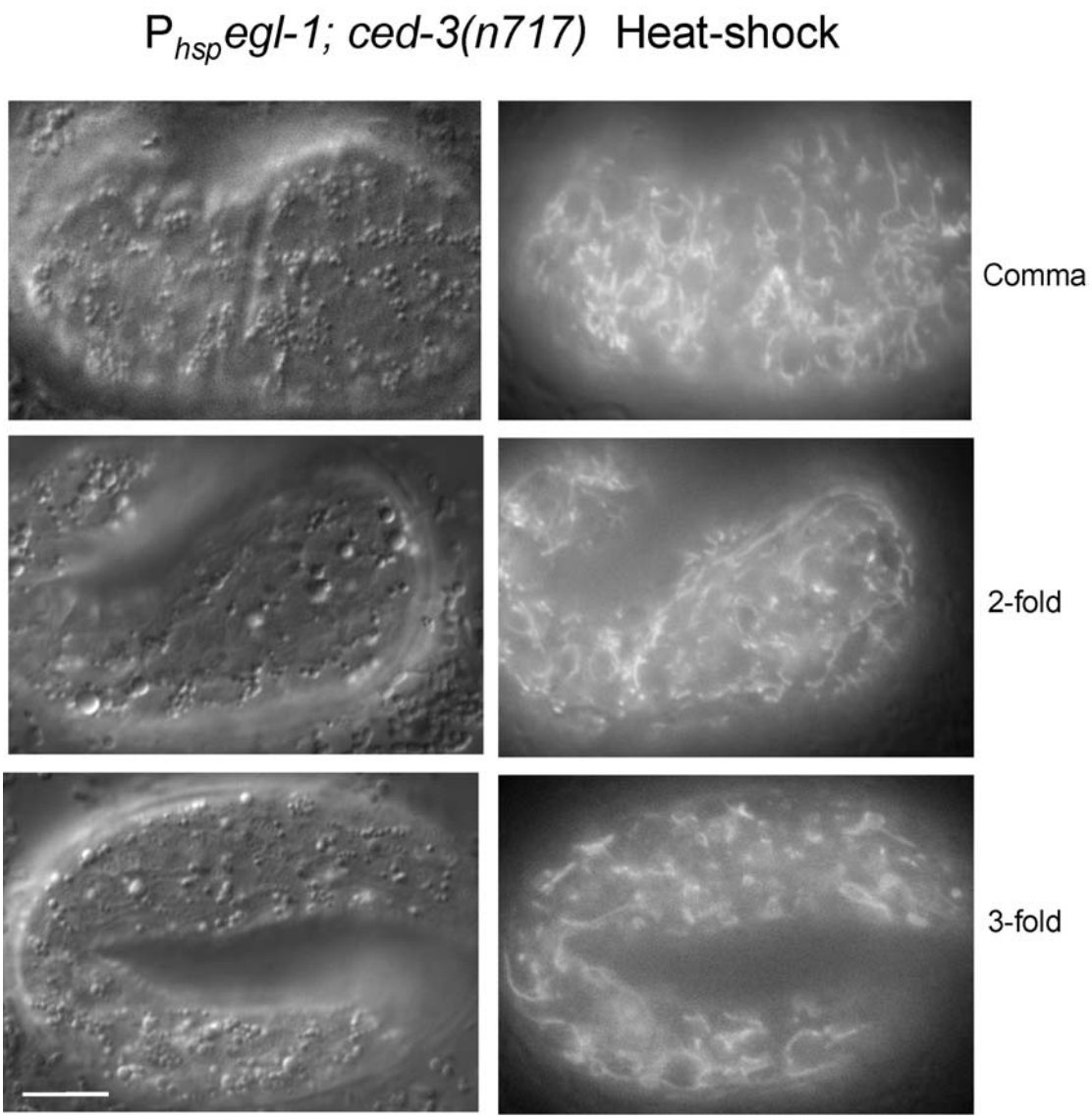

Figure S6. Ectopic expression of EGL-1 does not induce mitochondrial fragmentation in a strong *ced-3(n717) lf* background. TMRE stained P$_{hsp}$*egl-1*; *ced-3(n717)* embryos were heat-shocked and embryos were analyzed at the comma stage, 2-fold stage, and 3-fold stage of development (approximately 2, 3, and 4-5 hours post heat-shock treatment, respectively). Note that in all thee embryos mitochondria appear long and connected. Scale bar represents 10 μm.

Supplemental References

1. Brenner, S. (1974). The genetics of Caenorhabditis elegans. Genetics *77*, 71-94.
2. Riddle, D.L., Blumenthal, T., Meyer, B.J., and Preiss, J.R. eds. (1997). *C. elegans II* (Cold Spring Harbor, New York: Cold Spring Harbor Laboratory Press).
3. Stanfield, G.M., and Horvitz, H.R. (2000). The *ced-8* gene controls the timing of programmed cell deaths in *C. elegans*. Mol. Cell *5*, 423-433.
4. Hengartner, M.O., Ellis, R.E., and Horvitz, H.R. (1992). *Caenorhabditis elegans* gene *ced-9* protects cells from programmed cell death. Nature *356*, 494-499.
5. Jagasia, R., Grote, P., Westermann, B., and Conradt, B. (2005). DRP-1-mediated mitochondrial fragmentation during EGL-1-induced cell death in *C. elegans*. Nature *433*, 754-760.
6. Muller-Reichert, T., Hohenberg, H., O'Toole, E.T., and McDonald, K. (2003). Cryoimmobilization and three-dimensional visualization of *C. elegans* ultrastructure. J. Microsc. *212*, 71-80.